Nanoplasmonics FDTD Simulations Using a Generalized Dispersive Material Model

Ludmila J. Prokopeva,[1] Alexander V. Kildishev,[2*] Jieran Fang,[2] Joshua Borneman,[2] Mark D. Thoreson,[2,3] Vladimir M. Shalaev,[2] and Vladimir P. Drachev[2]

[1]Institute for Computational Technologies, Russian Academy of Sciences, Novosibirsk, Russia

[2]Birck Nanotechnology Center, School of ECE, Purdue University, West Lafayette, IN 47907 USA
[*]a.v.kildishev@ieee.org

[3]School of Advanced Optical Technologies, University Erlangen-Nürnberg, Erlangen, Germany

Abstract: This work deals with the use of our recent generalized dispersive material (GDM) model built on Pade approximants that is applied to FDTD simulations of nanoplasmonic structures. In particular, our original formulation is compared to the classical recursive-convolution technique for the Lorentz oscillator using a complex recursive accumulator. The proposed GDM model is then used to simulate the spectral response of an array of 2D gold nanoslits, and the results are successfully validated with frequency-domain solutions. Another simulation example shows the transmission, reflection, and absorption spectra obtained from 3D FDTD parallel calculations of a multi-layer semicontinuous metal film. The numerically simulated results are then compared to data obtained from the optical characterization of a semicontinuous film sample with the same topology, and a comparison of both results demonstrates a good fit. Each example uses a modulated incident pulse with a fixed carrier frequency and a Gaussian envelope.

Keywords: FDTD, Recursive Convolution (RC), Generalized Dispersive Material (GDM), Critical Points (CP).

1. Introduction

While frequency-domain simulations of nanophotonic structures composed of dispersive media may be adequate for most cases, certain physical phenomena can only be represented in the time domain. Simulations containing nonlinear effects stronger than a mild perturbation (up to and including saturation), as well as photomodification and other irreversible phenomena, require a time-domain description. In frequency-domain (FD) numerical methods, the data for dispersive material properties is taken as a discrete set of experimental entries; however, the implementation of the dispersion in time-domain methods requires an approximation of FD dispersion data with an analytical function. The most popular approach, well covered in the FDTD literature, e.g. [1], is to take this analytical dependency as a combination of Debye, Drude, Sellmeier, and Lorentz terms, which provides a good fit with the FD data for metal and dielectric media [2]. A more recent and more effective FD approximation (better fit and less computational cost) is obtained for a number of noble metals with the so called critical points (CP) analytical dispersion model [3,4]. However, the dispersive FDTD method is not fully investigated for that latter model. So far only a few papers have reported successful numerical simulations using an FDTD method in combina-

tion with auxiliary differential equation (ADE) or first-order recursive convolution (RC) techniques to implement a CP dispersion model [5,6]. This need has motivated work to implement higher-order RC methods, and it has generally resulted in a necessity for a universal approach to the implementation of different dispersion terms and different ADE and RC methods. The latter was accomplished in [7], where the dispersion is introduced with Pade approximants and the proposed, explicit scheme is resolved in a minimized number of flops while, also, having the ability to easily switch between different ADE and RC methods of first- and second-order accuracies.

In Section 2, we recapitulate the approach proposed in [7]; although we show that for RC methods the initial formulation [7] can be simplified with the introduction of *complex* recursive accumulators, provided that the aim is to obtain the simplest formulas for the higher-order RC methods. The drawbacks of using complex recursive accumulators for specific dispersion models are discussed. The discussion is important since all the classical publications of the RC methods for Lorentz media [1], [8-12] utilize complex accumulators and can be improved by using real functions as has been done in [7]. In Section 3, we show the results of 2D and 3D simulations performed with the proposed dispersive FDTD.

2. Dispersive FDTD

In this section, we discuss the implementation of the dispersion of permittivity for time-domain methods. We revise the techniques that give the most general approaches to incorporate a wide class of dispersion models while exploiting different ADE and RC numerical schemes.

A. Dispersive FDTD Revised

For simulations, we use the conventional FDTD method by Yee; however, the dispersion is introduced using the generalized dispersive material (GDM) model based on Pade approximants [7]. In this approach, the dispersive permittivity function is assumed to be given in the frequency domain in the form

$$\varepsilon(\omega) = \varepsilon_\infty - \frac{\sigma}{\iota\omega\varepsilon_0} + \sum_{i\in I_1} \frac{a_{0,i}}{b_{0,i} - \iota\omega} + \sum_{i\in I_2} \frac{a_{0,i} - \iota\omega a_{1,i}}{b_{0,i} - \iota\omega b_{1,i} - \omega^2}, \tag{1}$$

which includes the most important metal and dielectric dispersion models such as Drude-Lorentz, Debye, Sellmeier, and critical points. We will also need its transform to time domain, which is

$$\varepsilon\big(t\big) = \varepsilon_\infty\delta(t) + \sigma\varepsilon_0^{-1}U(t) + \sum_{i\in I_1} a_i e^{-\gamma_i t}U(t) + \sum_{i\in I_2} a_i e^{-\gamma_i t}\sin(\delta_i t - \varphi_i)U(t), \tag{2}$$

here, $a_i = a_{0,i}$, $\gamma_i = b_{0,i} \;\; \forall\, i \in I_1$ or $a_i = \delta_i^{-1}\sqrt{a_{0,i}^2 - a_{0,i}a_{1,i}b_{1,i} + b_{0,i}a_{1,i}^2}$, $\varphi_i = \mathrm{Arg}[a_{0,i} - a_{1,i}(\gamma_i + \iota\,\mathrm{Re}\,\delta_i)]$, $\gamma_i = \frac{1}{2}b_{1,i}$, $\delta_i = \sqrt{b_{0,i} - \gamma_i^2} \;\; \forall\, i \in I_2$, $\delta(t)$ is Dirac delta function, and $U(t)$ is Heaviside step function.

And the time-domain partial polarizations corresponding to term χ_i, and denoted as $\mathbf{P}_i$, satisfy the ODEs

$$\begin{array}{lll} \dot{\mathbf{P}}_i + b_{0,i}\mathbf{P}_i = a_{0,i}\mathbf{E}, & \mathbf{P}_i(0) = 0 & \forall i \in I_1 \\ \ddot{\mathbf{P}}_i + b_{1,i}\dot{\mathbf{P}}_i + b_{0,i}\mathbf{P}_i = a_{0,i}\mathbf{E} + a_{1,i}\dot{\mathbf{E}}, & \dot{\mathbf{P}}_i(0) = \mathbf{P}_i(0) = 0 & \forall i \in I_2 \end{array}, \tag{3}$$

where the components of the electric polarization vector **P** are normalized along with **E** and **H** fields by the incident field factors D_0, E_0, H_0, with $D_0 = \varepsilon_0 E_0$, $H_0 = \sqrt{\varepsilon_0\mu_0^{-1}}E_0$. The polarizations can be written through the convolution integral $\big(I = I_1 \cup I_2\big)$

$$\mathbf{P}_i(t) = \int_0^t \chi_i(\tau)\mathbf{E}(t-\tau)d\tau \;\; \forall i \in I\,. \tag{4}$$

Numerically, local polarization can be calculated using a finite-difference approximation of the ODEs (3) (ADE method) or by using the numerical integration of a convolution integral (4) (RC methods). As it is shown in [7], both numerical methods result in recurrences of the form

$$\mathbf{P}_i^{n+1} = \beta_{1,i}\mathbf{P}_i^n + \alpha_{2,i}\mathbf{E}^{n+1} + \alpha_{1,i}\mathbf{E}^n \quad \forall i \in I_1, \tag{5}$$

$$\mathbf{P}_i^{n+1} = \beta_{1,i}\mathbf{P}_i^n + \beta_{0,i}\mathbf{P}_i^{n-1} + \alpha_{2,i}\mathbf{E}^{n+1} + \alpha_{1,i}\mathbf{E}^n + \alpha_{0,i}\mathbf{E}^{n-1} \quad \forall i \in I_2. \tag{6}$$

For ADE methods, the coefficients $\alpha_{k,i}, \beta_{k,i}$ are found immediately after the finite-difference approximation of (3) and grouping terms. For RC methods, the derivation of the coefficients requires more algebraic effort. In [7], we give general formulas for coefficients $\alpha_{k,i}, \beta_{k,i}$, which are parameterized through the first two approximation coefficients of the numerical integration sum and apply to the formulas for five RC methods: TRC[8], PCRC2 [9], PLRC [10], RRC [11], and PCRC [12]. However, this algebraic effort can be simplified even more by using a complex exponential susceptibility for $i \in I_2$ terms (compare to (2))

$$\tilde{\chi}_i(t) = -\iota a_i e^{(-\gamma_i + \iota\delta_i)t - \iota\varphi_i} U(t) \quad \forall i \in I_2, \tag{7}$$

so that the actual polarization is $\mathbf{P}_i(t) = \mathrm{Re}\big[\tilde{\mathbf{P}}_i(t)\big]$, where $\tilde{\mathbf{P}}_i(\omega) = \mathbf{E}(\omega)\tilde{\chi}_i(\omega)$. The simplification is an obligatory trick in all basic publications of RC methods applied to the Lorentz dispersion model; however, it has some drawbacks. In the next subsections, the generalized approach [7] is formulated with complex susceptibility and the pros and cons of both real and complex RC realizations are discussed.

B. Using Complex Exponential Susceptibility for RC Methods

The starting point of this approach is the validity of the equation $\mathrm{Re}\big[\tilde{\chi}_i(t)\big] = \chi_i(t)$, $i \in I_2$, since this holds only if $\delta_i = \sqrt{b_{0,i} - \frac{1}{4}b_{1,i}^2} \in \mathbb{R}$, $i \in I_2$. The latter is equivalent to the condition that if the Drude or the over-damped Lorentz terms are present in the sum (1), they must be expanded to irreducible terms, that is to a conductivity term and Debye terms $i \in I_1$. Then, all partial susceptibilities $\chi_i(t)$, $i \in I_1$ and $\tilde{\chi}_i(t)$, $i \in I_2$ have the exponential representation $\alpha e^{\beta t}U(t)$, and the original lemma from [7] gives a recursive formula for all partial polarizations $\mathbf{P}_i(t)$, $i \in I_1$ and $\tilde{\mathbf{P}}_i(t)$, $i \in I_2$.

Lemma. If an RC approximation method for the exponential susceptibility $\chi(t) = \alpha e^{\beta t}U(t)$ is given with the sum $\mathbf{P}^n = \sum_{j=0}^{n-1}\chi_j\mathbf{E}^{n-j}$ and the approximation coefficients satisfy the recurrence $\chi_j = e^{\beta\tau}\chi_{j-1}$, $j \geq 2$, then the recursive rule for polarization can be written as

$$\mathbf{P}^{n+1} = e^{\beta\tau}\mathbf{P}^n + \chi_0\mathbf{E}^{n+1} + \big[\chi_1 - \chi_0 e^{\beta\tau}\big]\mathbf{E}^n. \tag{8}$$

Table 1: RC Coefficients for exponential pole $\chi(t) = \alpha e^{\beta t}U(t)$

	2nd Order RC Methods, $\chi_k = e^{\beta\tau}\chi_{k-1}, k \geq 2$			1st Order RC Methods, $\chi_k = e^{\beta\tau}\chi_{k-1}, k \geq 1$	
	TRC [8]	PCRC2 [9]	PLRC [10]	RRC [11]	PCRC [12]
χ_0	$\frac{1}{2}\alpha\tau$	$\alpha\beta^{-1}\left(e^{\beta\tau/2} - 1\right)$	$\alpha\beta^{-2}\tau^{-1}(e^{\beta\tau} - 1 - \beta\tau)$	$\alpha\tau$	$\alpha\beta^{-1}\left(e^{\beta\tau} - 1\right)$
χ_1	$\alpha\tau e^{\beta\tau}$	$\alpha\beta^{-1}\left(e^{\beta\tau} - 1\right)e^{\beta\tau/2}$	$\alpha\beta^{-2}\tau^{-1}\left(1 - e^{\beta\tau}\right)^2$	-	-

In particular, this lemma gives a recursive integration formula for methods such as RRC, TRC, PLRC, PCRC, and PCRC2; the coefficients χ_0, χ_1 for all listed methods are given in Table 1.

Finally, we incorporate the permittivity function (1) into Yee's FDTD scheme through polarizations:

$$\varepsilon_\infty(\mathbf{E}^{n+1} - \mathbf{E}^n) + \frac{\sigma\tau}{2\varepsilon_0}(\mathbf{E}^{n+1} + \mathbf{E}^n) + \sum_{i\in I_1}(\mathbf{P}_i^{n+1} - \mathbf{P}_i^n) + \mathrm{Re}\sum_{i\in I_2}(\tilde{\mathbf{P}}_i^{n+1} - \tilde{\mathbf{P}}_i^n) = c\tau(\nabla\times\mathbf{H})^{n+1/2}. \tag{9}$$

Formulas (8)-(9) are additionally rearranged to minimize the number of performed flops:

$$\begin{cases} \mathbf{E}^{n+1} = \xi_1^{-1}\left[\xi_0\mathbf{E}^n - \mathrm{Re}\sum_{i\in I}\Psi_i^n + c\tau(\nabla\times\mathbf{H})^{n+1/2}\right], \\ \Psi_i^{n+1} = e^{\beta_i\tau}\Psi_i^n + \chi_{1,i}(e^{\beta_i\tau}-1)\mathbf{E}^n, \ \forall i\in I \end{cases} \tag{10}$$

with

$$\xi_1 = \varepsilon_\infty + \frac{\sigma\tau}{2\varepsilon_0} + \mathrm{Re}\sum_{i\in I}\chi_{0,i}\,,\ \xi_0 = \varepsilon_\infty - \frac{\sigma\tau}{2\varepsilon_0} + \mathrm{Re}\sum_{i\in I}(\chi_{0,i}-\chi_{1,i})\,. \tag{11}$$

One can easily reproduce the formulas (10)-(11) utilizing $\Psi_i^n = \mathbf{P}_i^{n+1} - \mathbf{P}_i^n - \chi_{0,i}\mathbf{E}^{n+1} + (\chi_{0,i}-\chi_{1,i})\mathbf{E}^n$.

Using (11), with coefficients χ_0, χ_1 from Table 1 and the exponential representation for susceptibilities (2)-(7), the dispersion implementation of most RC methods becomes straightforward, including implementation of the Debye, Drude, Lorentz and critical points models.

C. Disadvantages of the Approach with Complex Exponential Susceptibility

The obvious advantage of using the complex recursive accumulators is the relative ease of the numerical formulas. However, for that advantage we pay with the following drawbacks:

a) The update of each complex recursive accumulator is done in 10 flops; however, by converting the complex-valued formulas into real functions, the same procedure can be performed in 7 flops (see [7]);
b) The complex recursive formula is not suitable for the analysis of numerical aspects of the method, such as stability and dispersion; in that case conversion to real functions is required;
c) The over-damped Lorentz and Drude terms must be expanded to Debye and conductivity terms.

3. Numerical simulations

To verify our method, we investigated the optical properties of gold and silver nanostructures. The dispersive function of gold is more precisely defined as a sum of a Drude term and two critical points terms (D2CP). For silver, which is examined in the wavelength band above the interband transitions, we may use the Drude model. The detailed functions and parameters for these models are described in [13].

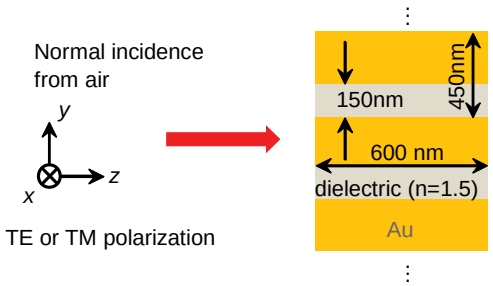

Fig. 1. 2-D simulation model with gold nano-slits.

A. 2-D Simulation with Gold Nano-Slits

First, we examine a 2-D simulation with periodic gold nano-slits under normal incidence of TE- or TM-polarized waves, as shown in Fig. 1. The gold slits are surrounded by air and extend to infinity in the x direction. All of the 150-nm slits are made in a 600-nm silver film with a 450-nm period; the slits are filled with a dielectric material (refractive index, $n = 1.5$). The rectangular simulation domain is set to be 10 μm in the z direction, with perfectly matched layer (PML) truncation at the two sides that are perpendicular to this direction, and 450 nm in the y direction with periodic boundary conditions (PBC) applied to the remaining sides to mimic a periodic array of infinitely extended slits. The spatial step is 5 nm (the Courant condition number is 0.5). To obtain the broadband response, we take the incident E-field to be a Gaussian pulse (300-nm carrier, 237~408-nm FWHM, 3-fs offset). The field probes, which are located close to the source and the shade sides along the longitudinal (propagation) direction, are then post-processed with FFT to obtain the numerical reflection and transmission spectra. The results are compared

to a semi-analytical tool based on the spatial harmonic analysis (SHA) method and freely available online [14]. As shown in Fig. 2, the reflection and transmission spectra for both TE and TM polarizations are in excellent agreement; the absolute numerical errors are within the range of 0.01 across the whole wavelength range from 500 to 1600 nm.

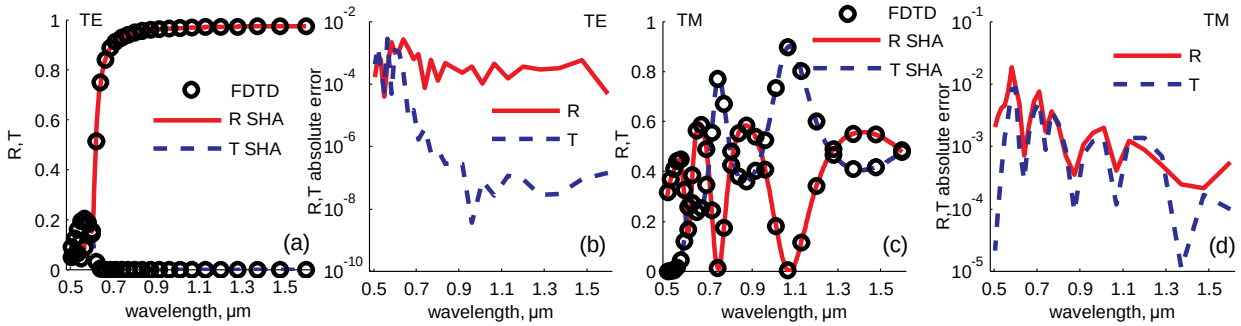

Fig. 2. Comparison of transmission-reflection spectra of 2-D gold slits, (a) TE polarization and (b) its absolute error, (c) TM polarization and (d) its absolute error.

B. 3-D Simulations with Multi-Layer Composite Ag/SiO_2 Film

Our other important example deals with the spectral responses of a multi-layer, composite Ag/SiO_2 film on a glass substrate ($n = 1.52$). As illustrated in Fig. 3(a), the input model for the composite film is generated by converting the FE-SEM image of a fabricated film (Figure 3(b)) to a binary image, where an appropriate grayscale threshold is used to determine the locations occupied by silver and SiO_2 ($n = 1.45$). It is impossible to model the entire area of the film; therefore, the complete film image is divided into individual frames (200×200 nm^2 each). The spatial step is 2 nm (the Courant condition number is 0.5). The PML-truncated simulation domain is 4 μm long. PBCs are applied to all sides parallel to the z direction.

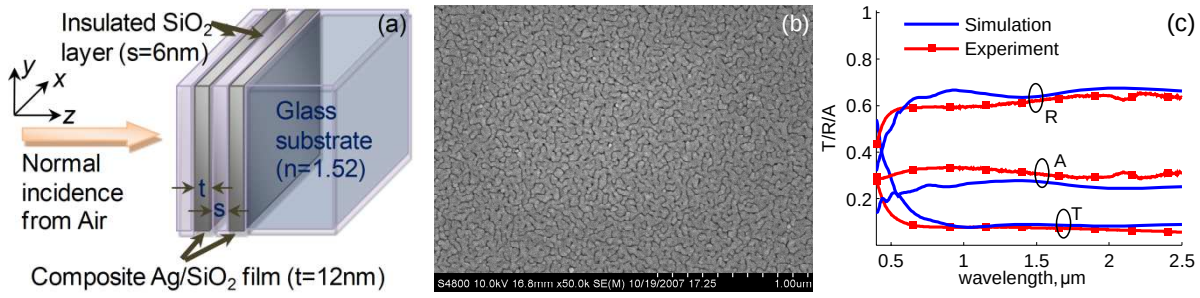

Fig. 3. FDTD simulation of a multi-layer composite Ag/SiO_2 film deposited on a thick glass substrate.

The calculated spectra change widely from frame to frame due to differences in geometry; hence, to obtain statistically sound average spectra of the film, we calculated a representative number of individual spectra [15,16]. Fig. 3(c) depicts the averaged reflection (R), transmission (T) and absorption (A) spectra, which are in good agreement with the experimental data (assuming a stochastic topology of the film, and simplifications introduced by averaging the spectra of periodically arranged finite-sized frames).

4. Conclusions

We apply the generalized dispersive material model [7], based on the Pade approximants of the dispersive dielectric function for two-dimensional and three-dimensional simulations of nanoplasmonic structures. This method is used due to its ability to work uniformly with different dispersion terms such as Drude, Lorentz, Debye, critical points, and Sellmeier, and to easily switch between ADE and RC methods, while having the same or better effective performance.

The approach used was compared to the classical RC treatment of conjugate poles with complex accumulators. We showed that although using complex functions simplifies the derivation of the scheme coefficients for RC methods, it has a number of drawbacks with respect to the method given in [7].

The two-dimensional validation simulations were performed with periodic gold slits, for which the dispersion of permittivity was described with the critical points model. The verified transmission/reflection spectra show good agreement with the spatial harmonic method. Then the method was applied to three-dimensional simulations of random films, where the economy on flops with a better realization of dispersion is the most important for the overall performance of the FDTD method.

Acknowledgement

This work was partially supported by ARO MURI 56154-PH-MUR, 50342-PH-MUR, and also through IIP SB RAS No 113, and RFFS No 09-01-00352-a.

References

[1] A. Taflove, S. C. Hagness, *Computational Electrodynamics: The Finite-Difference Time-Domain Method,* Artech House, 2005.

[2] F. Hao, P. Nordlander, "Efficient dielectric function for FDTD simulation of the optical properties of silver and gold nanoparticles," *Chem. Phys. Lett.*, Vol. 446, pp. 115-118, 2007.

[3] A. Vial and T. Laroche, "Comparison of gold and silver dispersion laws suitable for FDTD simulations," *Appl. Phys. B*, Vol. 93, pp. 139-143, 2008.

[4] P. Etchegoin, E. Le Ru, M. Meyer, "An analytic model for the optical properties of gold," *J. Chem. Phys.*, Vol. 125, pp. 164705-3, 2006.

[5] A. Vial, "Implementation of the critical points model in the recursive convolution method for modelling dispersive media with the finite-difference time domain method," *J. Opt. A: Pure Appl. Opt.*, Vol. 9, pp. 745-748, 2007.

[6] J. Lu and Y. Chang, "Implementation of an efficient dielectric function into the finite difference time domain method for simulating the coupling between localized surface plasmons of nanostructures," *Superlattice Microst.*, Vol. 47, pp. 60-65, 2009.

[7] L. J. Prokopeva, J. Borneman, and A. V. Kildishev, "Optical dispersion models for time-domain modeling of metal-dielectric nanostructures," *IEEE T. Magn.* (to be published).

[8] R. Siushansian, J. LoVetri, "A comparison of numerical techniques for modeling electromagnetic dispersive media," *IEEE Microw. Guided W.*, Vol. 5, pp. 426-428, 1995.

[9] J. W. Schuster, R. Luebbers, "An accurate FDTD algorithm for dispersive media using a piecewise constant recursive convolution technique," *IEEE Antennas Prop.*, Vol. 4, pp. 2018-2021, 1998.

[10] D. F. Kelley, R. Luebbers, "Piecewise linear recursive convolution for dispersive media using FDTD," *IEEE T. Antenn. Propag.*, Vol. 44, pp. 792-797, 1996.

[11] R. J. Hawkins, J. S. Kallman. "Linear Electronic Dispersion and Finite-Difference Time-Domain Calculations: A Simple Approach," *J. Lightwave Technol.*, Vol. 1, pp. 1872-1874, 1993.

[12] R. Luebbers, F. Hunsberger. "FDTD for Nth-order dispersive media," *IEEE Trans. Antennas Propag.*, Vol. 40, pp. 1297-1301, 1992.

[13] X. Ni, Z. Liu, and A. V. Kildishev, "PhotonicsDB: Optical Constants," doi: 10254/nanohub-r3692.10, 2007.

[14] X. Ni, Z. Liu, F. Gu, M. G. Pacheco, J. Borneman, and A. V. Kildishev, "PhotonicsSHA-2D: Modeling of Single-Period Multilayer Optical Gratings and Metamaterials, " doi: 10254/nanohub-r6977.9, 2009.

[15] U. K. Chettiar, P. Nyga, M. D. Thoreson, A. V. Kildishev, V. P. Drachev, and V. M. Shalaev, "FDTD modeling of realistic semicontinuous metal films," *Appl. Phys. B*, Vol. 100, pp. 159-168, 2010.

[16] M. D. Thoreson, V. P. Drachev, J. Fang, A. V. Kildishev, L. J. Prokopeva, P. Nyga, U. K. Chettiar, and V. M. Shalaev, "Fabrication and Realistic Modeling of 3D Metal-Dielectric Composites, " *J. Nanophotonics* (to be published).